Advances in CFD & Actuator Disk Models for Helicopter Aerodynamics

Antonio Filippone[1] and Robert Mikkelsen[2]

[1]*School of MACE, The University of Manchester, Manchester, UK.*
[2]*Dept. of Mechanical Engineering, DTU, Lyngby, Denmark.*

Abstract

This contribution describes a new computational model for the aerodynamic flows past a complete helicopter in- and out of ground effect. The model is based on an unsteady RANS code, coupled with an actuator disk and blade element method for the rotors. The implementation does not specifically require any changes in the computational mesh due to the presence of the rotor disk, an item of interest in other methods. The effect of the rotor is modelled iteratively as a momentum source distribution, which is the main novelty of this contribution. The disk loading is calculated with a convolution through a Gaussian function. Examples of results are shown for an airframe in low-speed forward flight in proximity to the ground (ground clearance h/d = 0.8).

1. Introduction

The helicopter airframe is a bluff body that can only be partly streamlined. Knowledge gained in the past twenty years or so has already been applied in some cases to flow control of the fore-body and the after-body, and has greatly improved the aerodynamic performance of the airframe. However, in many cases the design constraints (payload, fuel tanks, operational items, etc.) do not allow much flexibility. In aggregate, the amount of drag created by the fuselage can exceed 40% of the total drag, depending on flight conditions.

Another source of concern arises from the fact that the helicopter airframe operates at virtually all angles of attack (from vertical climb to vertical descent) and a wide range of yaw angles (due to trim requirements, operational manoeuvres, side gusts, etc.). In ground effect (mostly at take-off and landing), the airframe finds itself constrained between a solid surface and the main rotor disk. In some cases, helicopters also operate from inclined surfaces, near large buildings and other near-side objects.

A correct evaluation of the influence of the fuselage is important on several aspects: 1.) in vertical flight it gives rises to a downwash that causes an increase in power requirements; 2.) in ground effect there is the problem of flow recirculation (fountain effect) with consequences on the rotor power requirements, on the stability of the aircraft and the ingestion of dirt/dust by the engine intakes; 3.) in forward flight, the aerodynamic performance of the fuselage has consequences on the lateral and longitudinal stability of the aircraft, particularly in those cases when the trim requirements lead to a yawed flight. Starting from this set of issues in the aero-flight mechanics of the rotorcraft, research has been initiated to develop suitable computational models to calculate the fuselage under some typical flight conditions.

Thus, the bluff body is required to operate at optimal conditions at points of the envelope that are not even considered for a fixed-wing aircraft. This operational complexity, coupled with the unsteady three-dimensional nature of the aerodynamic flows, makes the calculations of the airframe an item of interest both at the design stage and in the operational field. Helicopter aerodynamic calculations generally focus on the main rotor or the fuselage alone. Only recently there have been attempts to consider the integration between the two systems, with is of greater complexity than the sum between two items. In fact, the critical point is the rotation of the blades with respect to the airframe. This problem has been solved in a number of ways, for example by using Chimera grids, which are partly overlapping. The use of actuator disk theories has proven particularly advantageous. For example, there is no need for a full unsteady rotor calculation, and the problem is reduced to the iterative solution of a disk loading, at a far less computational cost. By comparison, methods that include a Chimera grid for the main rotor require several rotor revolutions, small time-steps and consequently very large computer resources. Extensive research on fuselage CFD has been presented in recent years (for example, Le Chuiton [1], Khier [2] and Schweikhard [3]) that has addressed actuator disk modelling for a complete computational model of the helicopter. A practical disadvantage is that some of the details of the rotor environment are lost. However, a choice can be made. If the focus is on the rotor, the costs of the complications cannot be avoided. If, instead, the focus is on the fuselage, methods based on the actuator disk offer considerable advantages.

Alternative numerical algorithms have been developed in recent years to make progress in helicopter airframe calculations. These methods include Detached-Eddy-Simulations (DES), Large-Eddy Simulations, and Implicit LES. All these methods require considerable hardware resources. However, most of the methods rely on some sort of simplifications for the rotor, one of which is the actuator disk model. The grid strategy is always more complicated in the presence of the rotor, not only because of the rotation of the blades. One method that has been applied with success is a Chimera grid.

Among these methods, we now propose a new numerical procedure, one that does not require any change at all on the integration domain, except for internal boundary conditions. This paper addresses the problem of coupling the CFD for fuselage aerodynamics with an actuator disk model. Out scope include the simulation of helicopter wakes in confined spaces (with ground effect or otherwise). The approach proposed is novel in that the numerical model does not require to create a mesh to suit the actuator disk model. Thus, once a suitable mesh is created for the CFD solver, the actuator disk – boundary element method and field solution are all coupled together. The coupling is done via a distribution of momentum sources, according to the procedure briefly described below.

2. Actuator Disk with CFD Solver

The numerical actuator disk considered is in a polar frame of reference represented by 20 to 50 equidistant azimuthally distributed non-rotating lines with 20 to 50 points distributed in the radial direction along each line. At each point on each line, the local velocity triangle is derived from the computed velocity field at each time step/iteration. Velocities are calculated from linear interpolation between the cell velocities of the cell containing line points. Aerofoil data combined with the blade geometry of the rotor (chord, twist) are applied in a lifting line and blade-element method in order to compute blade/disk loading. Thus, the simulations are performed in a fully unsteady coupled manner with respect to the flow development. However, the loading on the disk is computed locally in a quasi-steady manner. For this reason, a full aero-elastic simulation is not feasible with the present formulation of the actuator disk. However, a stall delay modelling may be applied.

The computational grid is a Cartesian type grid and the polar loadings, $\mathbf{F}_{r\theta z}$ are transformed to equivalent Cartesian $\mathbf{F}_{xyz}$ load components in the disk system. Finally, the loading in the disk system is converted into the flow domain system $\mathbf{X}$ (X,Y,Z) by

$$\mathbf{F}\,(F_X, F_Y, F_Z) = (\mathbf{F}_{xyz}\cdot \mathbf{N}_x,\ \mathbf{F}_{xyz}\cdot \mathbf{N}_y,\ \mathbf{F}_{xyz}\cdot \mathbf{N}_z) \quad (1)$$

where $\mathbf{N}$ are the eigenvectors of the disk in the domain reference system. The computed disk loading is applied to the CFD mesh using a convolution with a Gaussian function (see Sørensen et. al. [4]), that serves as smearing function for the applied loading. Thus, the loading is concentrated at the disk position with the one-dimensional Gaussian function in the direction normal to the disk defined by

$$S_F = \frac{1}{2\varepsilon\sqrt{\pi}} \exp\left[-\frac{z_l^2}{\varepsilon^2} \right] \qquad (2)$$

where ε should be of the order of the local grid size. Here, z_l is the distance between cell-centred mesh points and the equivalent normal disk point. A three-dimensional Gaussian smearing may also be applied, in which loading is smeared spherically from each point on the disk. Inboard at the centre of the disk the one-dimensional smearing should be used. The three-dimensional smearing is not feasible at the centre of the rotor, since the tangential component is cancelled out by the three-dimensional smearing. Towards the tip or edge of the disk, a blend between a one-dimensional and convolution ensures a smooth load distribution there. The general idea of applying the convolution is to distribute loading on more than one cell, thereby avoiding singular behaviour.

3. CFD Solver

The flow solver used is the code EllipSys3D, that was designed for external and internal aerodynamic flows over a variety of applications [5,6,7]. The flow solver is optimised for message-passing interface (MPI) and is capable of running efficiently on multi-processor computers. Computations for this work have been done on multi-processor Linux clusters at the Technical University of Denmark and at the *Hector* National Supercomputing Facility in the UK.

The convective terms of the equations are discretized using a third-order QUICK upwind scheme and central differences are used for remaining terms. The pressure and velocity coupling is obtained with the SIMPLE algorithm. The momentum equations are solved by using a predictor-corrector method to advance the solution in time. The momentum equations are solved by using a red/black Gauss-Seidel point solver. The solution of the elliptic Poisson system arising from the pressure correction equation is accelerated using a multi-grid method. Three grid levels have been used for the results shown.

3.1. Mesh Generation

Figure 1 shows a side view of the mesh around the ¼-model scale of the *Dauphin* fuselage that operates in ground effect. The mesh is made of 284 blocks arranged in four layers, each block containing 16^3 cells, in total 1.1 million cells.

The actuator disk may be positioned and oriented arbitrarily inside the mesh, provided that sufficient mesh resolution is achieved at the disk location. Sufficient resolution is ensured by a near region of cells with equidistant type meshing about one rotor radius away from the fuselage. Outside the near region, grid lines are stretched away towards the half sphere domain boundaries. An inlet condition is applied at a slightly more than half of the sphere; outlet/zero normal gradients are applied to the remaining part of the sphere. A symmetry/slip or Euler condition is applied at the ground; no-slip walls are used on the fuselage. Thus, the wall boundary layers are resolved for turbulent computations. Turbulence is handled by using the *K-ω SST* model by Menter [8].

Computations are first carried out at steady state condition without the actuator disk. Next, computations are restarted from a converged solution and run in unsteady mode with the actuator disk switched on. Since the flow field is bound to separate below the fuselage in hover or ground-hover condition, the flow is naturally unsteady. The time-step for the calculations shown is set to 10^{-3} seconds.

4. Results and Discussion

The mesh is generated in a number of steps. First, multi-block surface mesh is built on the airframe. Then a volume mesh is calculated by using the ground as a physical boundary.

Due to the particular characteristics of the flow solver, all blocks are cubic, with the same number of cells in all directions. Calculations are presented for a helicopter in forward flight in ground effect, at flight speeds of 5 m/s and 20 m/s. The ground clearance is shown in Fig. 1, and corresponds to a rotor clearance *h/d* ~ 0.8. The rotor is scaled to ¼, as the airframe. The rotor model corresponds to the Eurocopter Dauphin AS365. The blades have ONERA sections OA2XX. The aerodynamic tables for these airfoils have been generated with the Xfoil code over a limited range of Mach numbers (M < 0.4) and then extrapolated to higher Mach number, following the method of Ref. [9]. The tabulated data for the aerodynamic coefficients are used as input for the blade-element method and the actuator disk model. An intermediate deck defines the position of the centre of the actuator disk, and the normal unit vector through the centre of the rotor.

4.1 Flight near the Ground at Low Speed

A first calculation was done at a low speed, which is in fact a more demanding case than a high-speed flight. This is due to the effects of the downwash and the change required to the far field conditions created by the rotor.

Figure 2 shows views of a computation in ground condition at an air speed U = 5m/s. The uneven loading applied to the grid appears as a smoothly distributed momentum sources although concentrated above the fuselage in a confined disk. The streamlines derived in the plane reveal the downwash and a vertical flow structure in front of the fuselage.

Figure 3 shows contours of the downwash velocities around the fuselage and an iso-surface of 10 m/s downwash velocity. The nature of the 3D streamlines through the rotor in revealed and below the fuselage, the upward velocities indicate the separated flow pattern there. The local streamlines in front of the helicopter show a recirculation zone, which is in fact characteristic of this flight regime. Thus, the method proves suitable for the prediction of various aspects of the aero-physics: the performance of the rotor, as well as the characteristics of the near wake, as affected by ground confinement.

4.2 Flight near the Ground at Medium Speed

Figure 4 displays the contours and the accelerated wake near the ground rear of the fuselage. Figure 5 shows pressure contours with regions of high pressure (stagnation) on top of the fuselage and at the ground.

Considering the flight at 20 m/s, the change in flow pattern near the surface is apparent from Fig. 4, dominated by the higher inflow velocity. Some asymmetry in the surface flow is visible when seen from above. The pressure contours indicate stagnation pressure in front and a smaller region of low pressure near the hub. The skin friction lines at 20 m/s and 5 m/s are compared in Fig. 5. The figure indicates the shift in pattern from low to high forward speed on the lower side of the airframe. In particular, there is more flow separation at low flight speed, as expected, as a result of the stronger downwash in comparison to the axial component of the air speed.

The thrust force history is shown in Fig. 6. This graph shows an unsteady trend after an initial transient, although it appears fairly stable at around 950N. The thrust was specified on the basis of the scaled model. In fact, since the model is at ¼ scale, the gross weight is scaled according to the law

$$W \cong x^{2.2} \qquad (3)$$

where x is the length of the model. Assuming that all the weight has to be supported by the main rotor, considering an average gross weight of about 3.5 tons for the full scale vehicle, the scaling law leads to a required thrust of the order of 1kN, in line with the result obtained. The axial velocity on the disk is shown in Fig. 7. At 5 m /s, the distribution appears rather uniform on most part of the disk whereas at 20 m/s the downwash is manly present in the aft region of the disk. The separated flow below the fuselage at 5m/s is also revealed in the irregular patterns of the skin friction lines below. The zero azimuth is at the bottom; the blades advance counter clockwise. Finally, Fig. 8 shows a comparison of effective angle of attack on the disk.

5. Conclusions

This initial study has demonstrated the capability of a new numerical model for the simulation of combined airframe and rotor aerodynamics, with or without ground effect. Progress has been achieved in the implementation of a complex computational model involving a URANS method, and actuator disk model for the rotor and a blade element theory. The coupling of these models is done through source terms within the volumes, and does not require substantial changes in the mesh topology. Examples of calculations have been shown at two forward speeds.

Some progress is clearly required in a number of areas, starting from grid refinements, analysis of the flow physics, complete validation of the model with experimental data, performance on the high-computing hardware platform. The model has the capability of modelling helicopter wakes in the general sense, although a detailed analysis of the near-wake is hindered by the intrinsic limitations of the lifting-line and blade element methods. However, progress in this area is possible, with the inclusion of dynamic stall models, for example.

Work is underway to evaluate the effects of the tail rotor on the overall flow characteristics. The addition of the tail rotor is done in the same fashion as the main rotor, through an intermediate deck that defines the centre of the rotor, the normal to the disk and the required thrust. The latter quantity is set from simple lateral trim conditions at the relevant flight state.

Post-processing of the data is another area of focus, since a typical computation produces a complex flow field, as partly shown in the figures presented. The data for the rotor performance are stored separately, hence it is possible to make an analysis of the actuator disk characteristics.

Acknowledgements

Part of this research has been performed under EPSRC Grant EP/F005954/1.

References

[1] Le Chuiton. *Actuator Disk Modelling for Helicopter Rotors*. Aerospace Science & Technology, **8**(4), pp. 285-297, 2004.

[2] Khier W. Time-accurate versus Actuator Disk Simulations of Complete Helicopters, pp. 209-220, in "High-Performance Computing in Science and Engineering 05", Springer, Berlin 2006.

[3] Schweikhard R. Actuator Disk for Helicopter Rotors in an Unstructured Flow Solver, *AHS Journal*, **52**(1), pp. 58-68, 2007.

[4] Sørensen J.N., Shen W.S. and Munduate X. Analysis of Wake States by a Full-field Actuator Disc Model. *Wind Energy* **1**(1), pp. 73-88, 1998.

[5] Michelsen J.A. Block-Structured Multigrid Solution of 2D and 3D Elliptic PDE's. Technical Report AFM 94-06, Technical University of Denmark, Dept of Mechanical Engineering, 1994.

[6] Filippone A. and Michelsen J.A. Aerodynamic drag prediction on helicopter fuselage. *J. Aircraft*, **38**(2), pp. 326-333, March 2001.

[7] Filippone A. Accurate aerodynamic prediction for helicopter airframes with high performance computing. *Aeronautical. J.*, **111**(1117), pp. 175-184, Oct. 2006.

[8] Menter FR. Two-Equation Eddy-Viscosity Turbulence Models for Engineering Applications. *AIAA J.* **32**(2), pp. 269-289.

[9] Filippone A. Rapid Estimation of Airfoil Aerodynamics for Helicopter Rotors, *J. Aircraft*, **45**(4), pp. 1468-1471, July 2008.

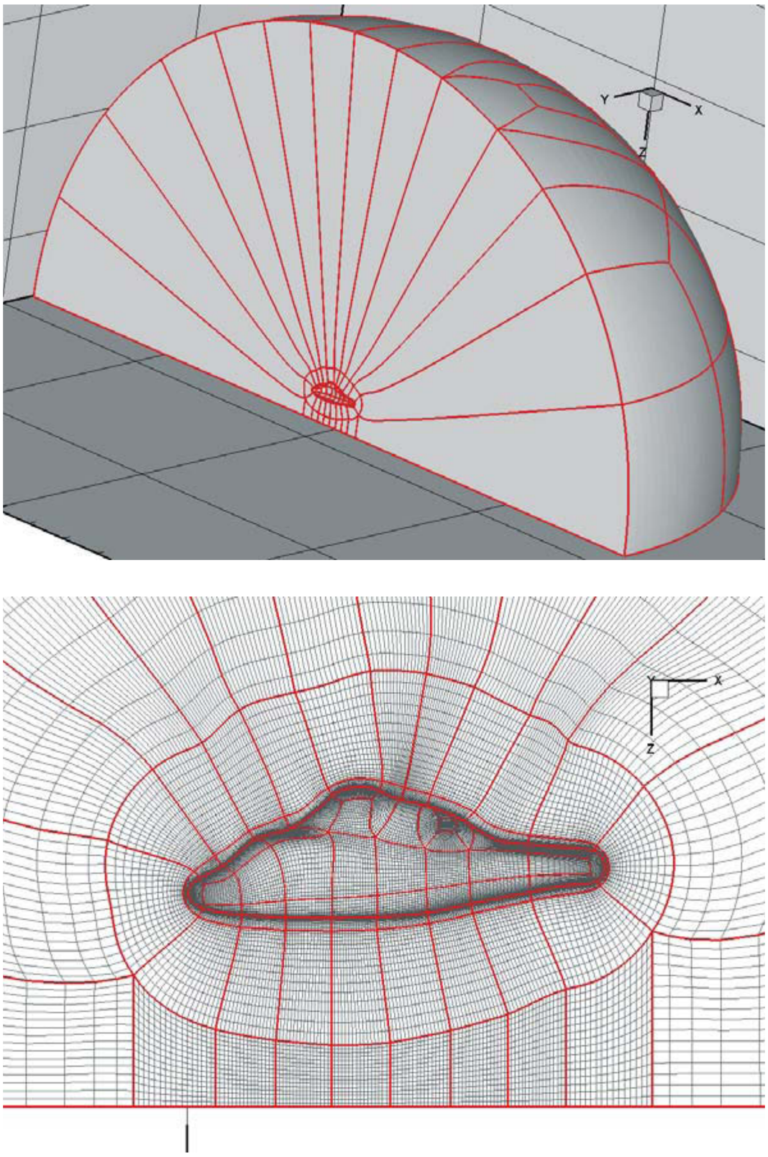

Figure 1. Mesh and block structure (top); computational domain (bottom); half model is shown.

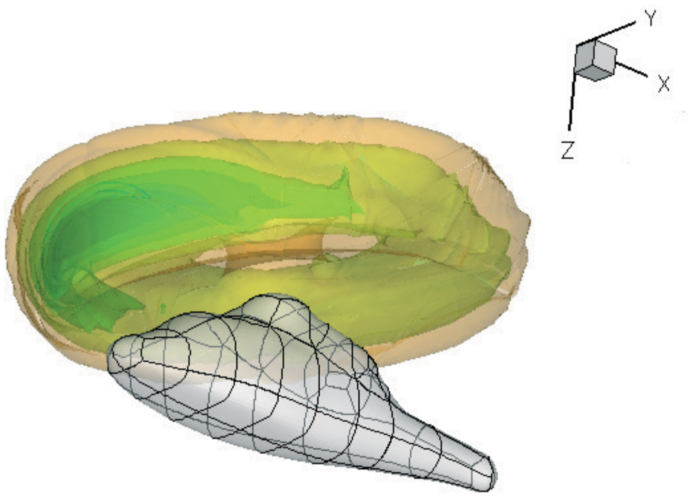

Figure 2: Helicopter in ground effect at 5m/s. Applied actuator disk loading.

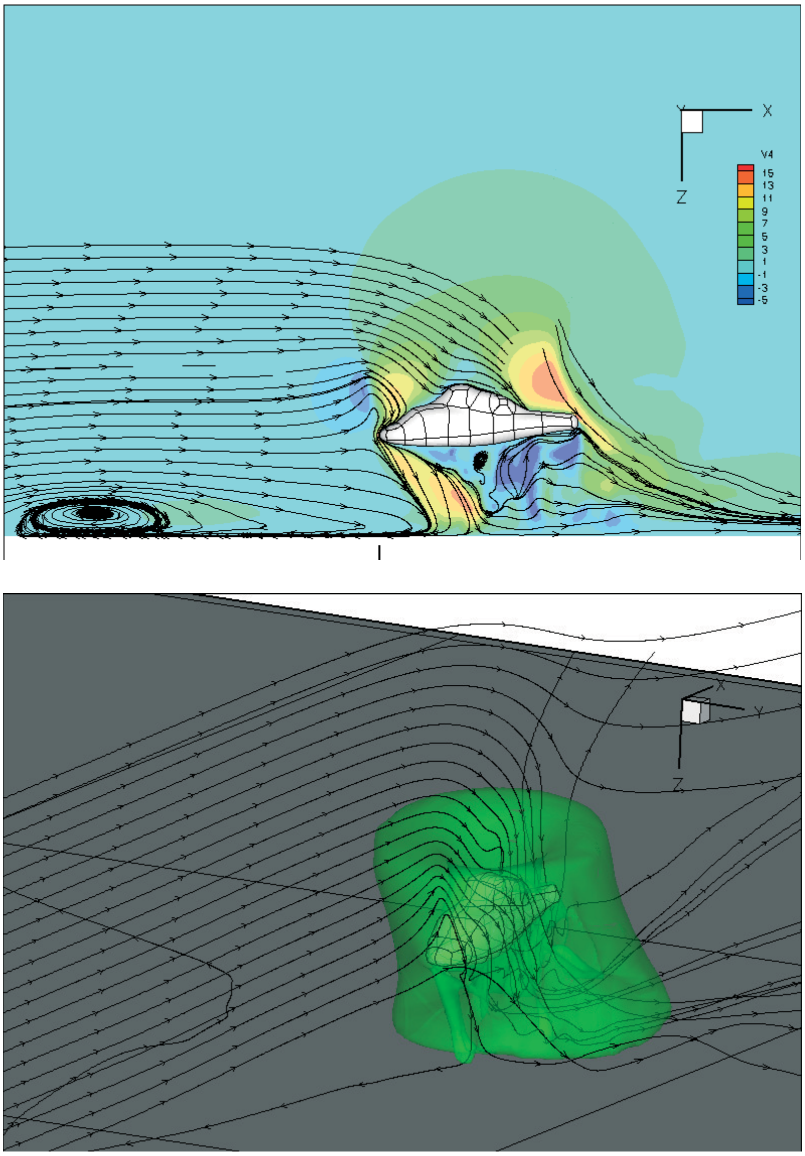

Figure 3: Downwash velocity contours (top) and planar streamlines at symmetry plane; iso-surface contour of 10m/s downwash velocity with 3D streamlines (bottom).

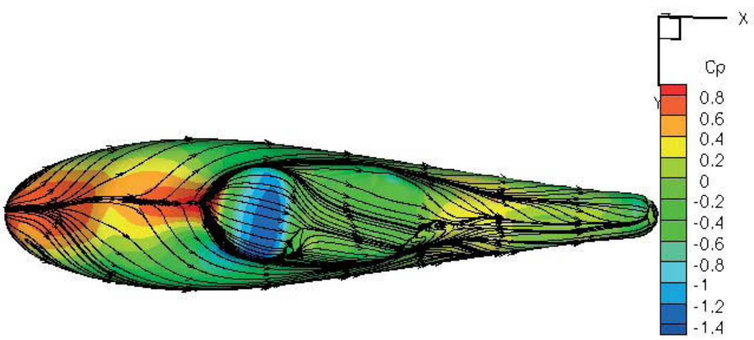

Figure 4: Forward flight at ground height, 20m/s. Surface skin frictions lines and pressure contours.

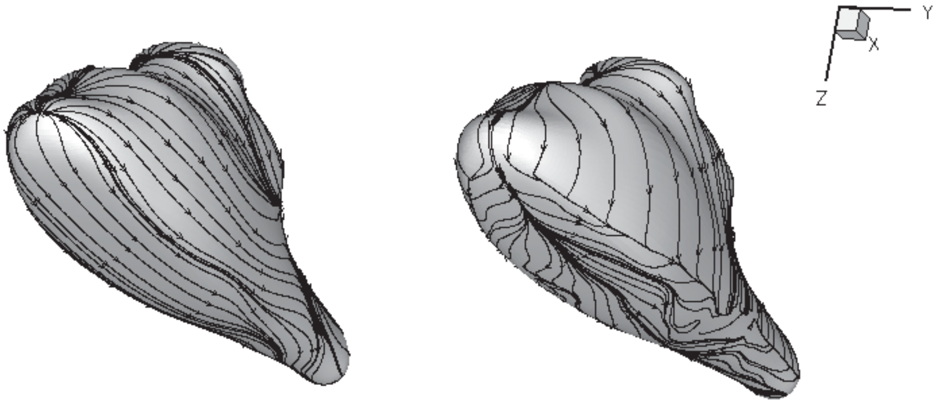

Figure 5: Skin friction lines seen from below, 20m/s (left) and 5m/s (right).

.

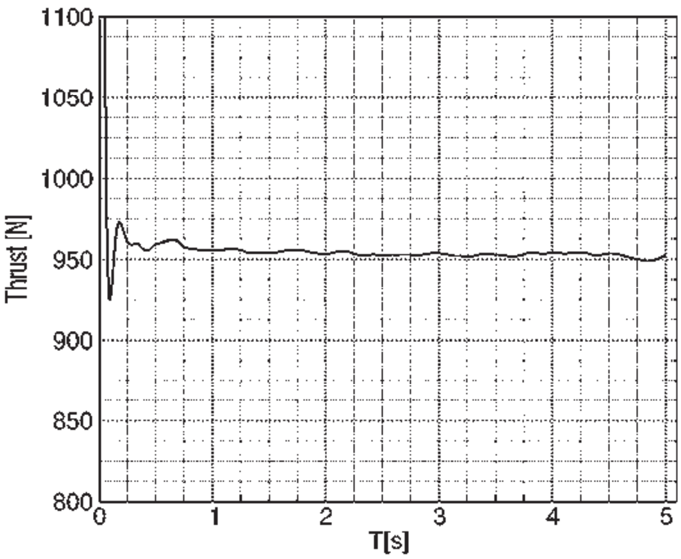

Figure 6: Time history of thrust force, 5 m/s.

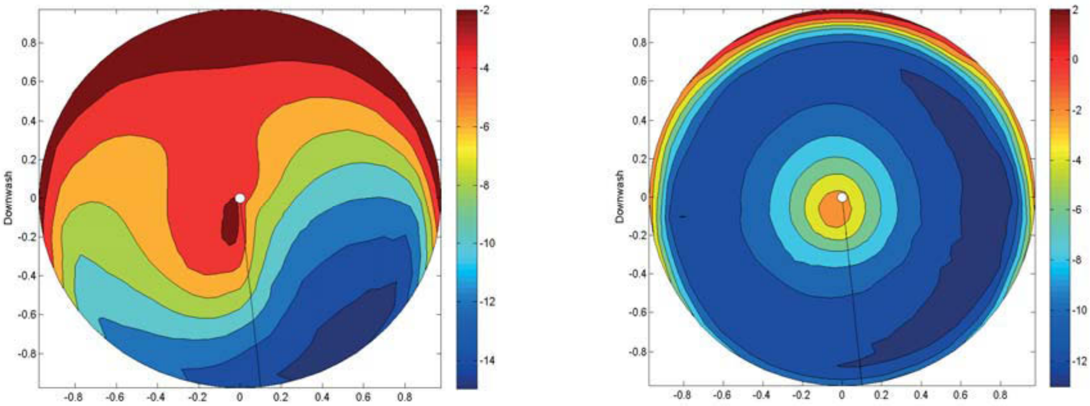

Figure 7: Axial velocity through the disk, 20m/s (left), 5m/s(right).

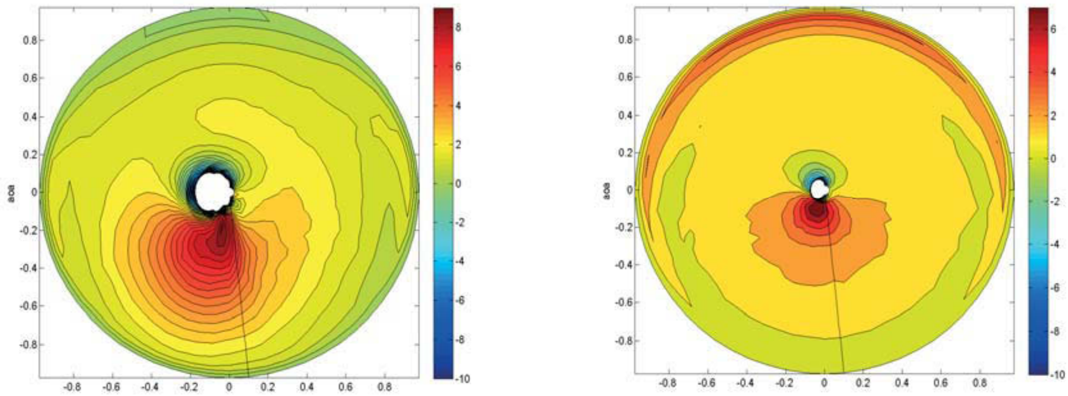

Figure 8: Local angle of attack, 20m/s (left), 5m/s (right).